

## 76. Drone-swarm based surveillance system for autonomous machine safety functionality

L. Nitti<sup>1</sup>, D. Bortoluzzi<sup>2</sup>, A. Biglia<sup>1</sup>, D. Ricauda Aimonino<sup>1</sup>, G. Torta<sup>2</sup>, G. Audrito<sup>2</sup>, F. Damiani<sup>2</sup>, P. Gay<sup>1,3</sup>, A. Rapp<sup>2</sup> and L. Comba<sup>1,\*</sup>

<sup>1</sup>DiSAFA – Università degli Studi di Torino, Largo Paolo Braccini 2, 10095 Grugliasco (TO), Italy; \*lorenzo.comba@unito.it

<sup>2</sup>Department of Computer Science (DI), University of Turin, Corso Svizzera 185, 10149 Torino (TO), Italy

<sup>3</sup>CNR-IEIIT, Corso Duca degli Abruzzi 24, 10129 Torino (TO), Italy

### Abstract

Drones and autonomous machines, both uncrewed aerial systems (UAS) and uncrewed ground vehicles (UGVs), are boosting precision agriculture, implementing remote sensing tasks as well as crop operations. Since the traditional collision avoidance systems can be limited to the sole routed inter-row path, to improve safety, additional monitoring systems can be envisaged. In this study, the effectiveness of deploying a UAS-swarm based surveillance system for UGV safety functionality is assessed by a simulation framework. Results showed that a system consisting of 3 UASs is an effective solution, proving a coverage of more than 80% of the area around the operating UGV.

**Keywords:** Agriculture 4.0, distributed control strategy, functional safety, swarm, uncrewed aerial system (UAS), uncrewed ground vehicle (UGV)

### Introduction

Currently, the adoption of UAS and UGV is leading to unprecedented innovation in precision agriculture practices (Rejeb *et al.*, 2022). This is particularly true in viticulture, a sector in which several commercial solutions, based on autonomous machines, are now available, supporting farmers in a wide range of tasks, including precise weeding, trimming or variable rate application of inputs (Mammarella *et al.*, 2022). These solutions are driving significant improvements in efficiency, precision, and sustainability of practices, ultimately enhancing grape quality and yield while minimizing the environmental impact. The automation of routine and labour-intensive tasks also addresses labour shortages and reduces operational costs.

Commercial autonomous machines embed several collision avoidance systems, such as LiDAR or ultrasonic sensors-based systems, which ensure the safety requirements by monitoring the area surrounding the machine, in particular along the direction of movement. However, while working within vine rows, the canopy extension can limit the FOV of the safety system to the sole routed inter-row path (Donati *et al.*, 2022). This can be risky when intrinsic operational hazards can involve obstacles/people in contiguous interrow paths, such as in the case of spraying operation (Biglia *et al.*, 2022a). Additional systems, with enhanced capability to monitor the machine surrounding area during operations, can increase the safety level of those autonomous solutions, and enable new, more critical, ones.

Enhancing safety requires additional systems capable of better monitoring the surrounding area. UAS equipped with cameras have been proven effective in covering large areas and detecting targets from advantageous viewpoints (Semsch *et al.*, 2009). These solutions have been applied, for example, in human detection for search and rescue missions. Sensors, including cost-effective RGB cameras or more advanced thermal cameras, have been adopted, using machine learning techniques to automatically process images and identify undesired elements. (Wang *et al.*, 2019)

In this study, the effectiveness of deploying a UAS-swarm based surveillance system for UGV safety functionality was assessed by a simulation framework, specifically developed for the case study. Each UAS (called safety UAS), equipped with a RGB camera, is intended to monitor a portion of the surrounding area (called safety area) around the working UGV (called operating UGV). The adoption of more than a single safety UAS, in a swarm scheme, was envisaged and investigated to ensure a total coverage of the area, overcoming the limits due to view occlusions due to 3D crops.

## Materials and methods

The simulation framework was based on two main modules, a first one devoted to compute the safety UAS trajectory with respect to the operating UGV, based on a decentralized control strategy, and a second module devoted to simulating the monitoring capability of the safety UAS swarm. To carry out a simulation, the framework developed requires the following input data: (i) a 3D model of a vineyard environment; (ii) the temporal evolution of the path of the operating UGV within the vineyard during a work mission; (iii) the characteristic of the safety area to be supervised and (iv) the number of UAS forming the swarm. At each discrete simulation time step, the outputs are: (a) the current safety area boundaries around the operating UGV; (b) the position of all the considered safety UAS; (c) the pose and (d) FOV of their cameras. From the output data, a set of performance indices of the whole swarm-based surveillance system can be computed, both at each time step and for the entire simulation. The simulation framework was implemented in Matlab (MathWorks, Natick, MA, USA) and C++ environments. Additional details are reported below.

### *Simulation input*

(i) 3D model of vineyard environment: the model of the vineyard environment has to be in the form of a triangulated mesh and highly detailed (Comba *et al.*, 2020). The 3D model can be generated by the structure from motion technique from aerial RGB images (Biglia *et al.*, 2022b). The model should be georeferenced in an absolute reference frame. In this work, a case study vineyard located in Piedmont, Northwest of Italy, was considered, which includes three contiguous parcels cultivated with Cv. Nebbiolo grapevine, covering a total surface of about 2.5 ha. The 3D model of the case study vineyard, generated with Agisoft Metashape (Agisoft, St. Petersburg, Russia) software from imagery acquired by a DJI Mavic Pro 2 (DJI Technology, Shenzhen, P.R. China), has a density of about 40 vertices/m<sup>2</sup> (Figure 1). For georeferencing purposes, 5 markers were placed in the vineyard during imagery acquisition, whose location was recorded with a Stonex S900 DGNN system (STONEX, Paderno Dugnano, Italy), with centimetric accuracy, at 1 Hz, in the UTM zone 32N reference frame.

(ii) Path of the operating UGV: it consists of the temporal evolution of the position coordinates of the operating UGV in a georeferenced frame. In this work, the path of a UGV during a sample working mission within the case study vineyard was recorded with a Stonex S900 DGNN system, with centimetric accuracy, at 1 Hz, in the UTM zone 32N reference frame.

(iii) Safety area: it is defined as the circular region around the operating UGV to be monitored by the UAS swarm. In this work, the radius of the safety area was set to 30 m, in compliance with recent spraying studies (Cech *et al.*, 2023).

(iv) Number of UAS: the simulation framework was implemented in order to be able to manage a different number of UAS scouts. In this work, a set of simulations have been undertaken, varying the number of safety UAS from 1 up to 5, in order to investigate their effect on the overall surveillance system performance, while serving the same working mission of the operating UGV.

### *Simulation modules*

(1) Safety UAS swarm control strategy: the swarm of UASs executes a fully distributed control algorithm based on the Aggregate Programming (AP) paradigm (Beal *et al.*, 2015), which has already been successfully applied in the simulation of robotic swarms (Aguzzi *et al.*, 2023). More

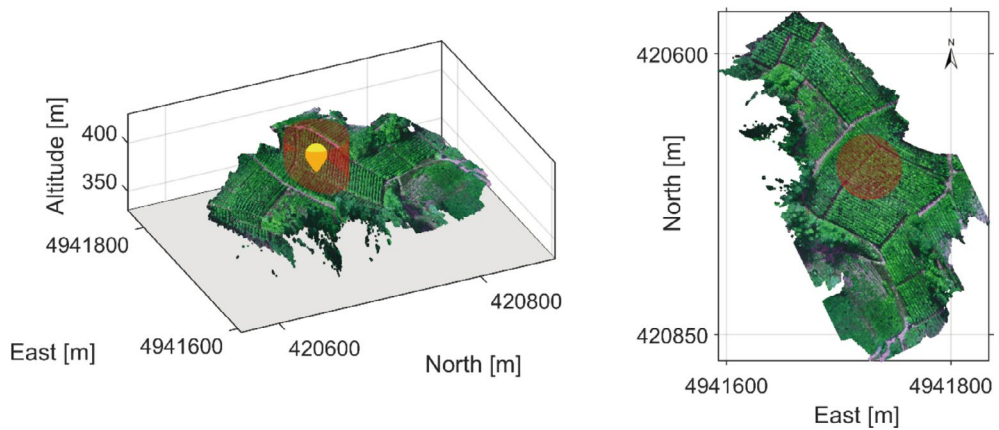


Figure 1. Graphical representation of the vineyard case study 3D model (on the left) and its top view (on the right), with a sample position of the operating UGV (yellow marker) and the safety area around it (red region).

specifically, each UAS is simulated as a device executing a C++ program enhanced with AP features through the FCPP library (Audrito, 2020). The goal of the distributed algorithm is to assign to each UAS a unique position along a circle centred in the current position of the UGV, obtaining a circular formation of UAS separated by equal arcs, with airborne camera orientation pointing to the operating UGV position. The UAS will then continuously aim to maintain this formation as the UGV moves along its trajectory. It is worth noting that the adoption of the AP paradigm, besides providing the coordination primitives for the distributed implementation of the outlined control strategy, also provides seamless robustness against the loss of UAS in the swarm (or the addition of new UAS): the adaptive nature of AP algorithms leads to an automatic re-arrangement of the UASs in an updated formation with fewer (or more) elements.

(2) Simulation of UAS FOV: the algorithm, developed in MATLAB environment, aims at simulating the portion of safety area properly monitored by the safety UAS, exploiting a rendering approach. Set the airborne cameras parameters (the angle of FOV, the resolution and the aspect ratio of the output image, the near and far plane distances), the camera view of each UAS was computed at each simulation step on the basis of their current pose. The camera view  $VCAM_i$  of the  $i$ -th UAS is in the form of a Boolean array, with length equal to the mesh faces number, and true values assigned to those faces successfully viewed by the UAS. The camera view is computed by the following step: (1) transformation of the mesh coordinates from the world to the camera frame, (2) selection of mesh portion within the simulated camera frustum, (3) the mesh portion transformation from the camera frame to the viewport frame, and (4) the rasterization process to obtain a simulated 2D image of the viewed portion of environment. Finally the camera view  $VCAM_i$  is filtered considering only those faces lying within the safety area.

In this case study, the camera parameters were those of the Hasselblad L1D-20c (Victor Hasselblad, Göteborg, Sweden) camera ( $77^\circ$  FOV angle, with a shooting range from 1 m to infinity, an output image resolution of  $5472 \times 3648$  pixels and an aspect ratio of 3:2), the sensor commonly mounted on DJI Mavic 2 and 2 Pro drones.

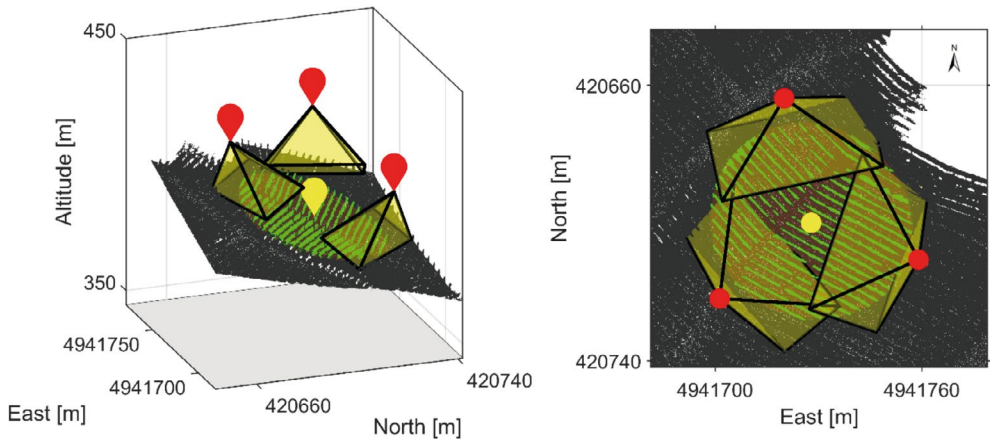


Figure 2. Plot of a portion of the vineyard case study 3D model (on the left) and its nadiral view (on the right), with the subset within the safety area (green and brown region), the position of the operating UGV (yellow marker) and safety UASs (red markers), along with their cameras viewing frustums (in yellow) during a sample simulation step of a 3 UAS swarm.

### Simulation output

- The safety area boundaries: the boundaries of the safety area define the portion of the mesh to be monitored by the swarm at the current simulation time step. This portion of the mesh is expressed as the indices of the mesh faces that lie within the safety area boundaries. The mesh subset, named SA, serves as reference to compute the system performance indices.
- The position of all the considered safety UAS: the positions of the safety UAS at the current simulation time step, expressed as UTM N, UTM E coordinates and altitude in the UTM zone 32N georeferenced frame.
- The pose of the safety UAS cameras: it is the orientation of the cameras equipped on each safety UAS with respect to the georeferenced frame.
- The camera view of each airborne sensor: the simulation outputs the rendered views by each safety UAS camera, as well as the indices of the successfully seen mesh faces within the safety area.

### Performance indices

To assess the performance of the safety system in terms of capability of monitoring coverage of the safety area and, in the meanwhile, to evaluate if the resources used (e.g. number of UAS) are not redundant, two performance indices were defined: coverage index  $I_c$  and the overlapping index  $I_o$ . For both the performance indices computation, the portion of the safety area seen by all the UAS forming the system is used, named  $V_{swarm}$ , defined as the union of all the subsets of mesh faces within the UASs as:

$$V_{swarm} = \bigcup_{i=1}^N V_{cam_i} \quad (1)$$

with  $N$  representing the overall number of UASs in the swarm. The coverage index was defined as the ratio between  $t$  and the overall region within the safety area to be monitored as:

$$I_c = \frac{V_{swarm}}{SA} \quad (2)$$

For the computation of the overlapping index, the portion of model seen more than once by the safety UAS is required, which is defined as:

$$V_{\text{over}} = \bigcup_{a,b \in \{1, \dots, N\}, a \neq b} (V_{\text{cam}_a} \cap V_{\text{cam}_b}) \quad (3)$$

The overlapping index is thus defined as:

$$I_o = \frac{V_{\text{over}}}{V_{\text{swarm}}} \quad (4)$$

The coverage index  $I_c$  reflects how effectively the UAS swarm is able to monitor the defined safety area around the operating UGV, while the overlapping index measures redundancy in coverage, i.e., how much of the area is seen by more than one UAS. The aforementioned indices are calculated at each simulation time step. The overall performance of the system was computed on a complete simulation, and the results were expressed as indices averages and standard deviation.

## Results

The performance of the UAS-swarm surveillance system in terms of coverage and overlapping indices was evaluated performing a simulation of more than 500 iteration steps for each number of safety UAS in the swarm, ranging from 1 to 5 UAS. The results from the simulation are summarized in Table 1 and Figure 3, which report the mean and standard deviation of both the coverage  $I_c$  and overlapping  $I_o$  indices for different swarm sizes. The mean values for  $I_c$  increases gradually from 32.42% (at  $N=1$ ) to 91.15% (at  $N=5$ ). Similarly, also  $I_o$  increases as more safety UASs are introduced, from 10.72% ( $N=2$ ) to 77.55% ( $N=5$ ). The standard deviation for  $I_c$  starts at 3.93% for  $N=1$  and decreases steadily as  $N$  increases, suggesting that the performance index becomes more stable as  $N$  progresses.

Table 1. Mean ( $\mu$ ) and standard deviation ( $\sigma$ ) of the performance indices  $I_c$  and  $I_o$  expressed in percentage for each UAS-swarm size simulated.

N	Coverage index $I_c$		Overlapping index $I_o$	
	$\mu$ (%)	(%)	$\mu$ (%)	(%)
1	32.42	3.93	–	–
2	64.74	2.10	10.72	2.63
3	83.65	2.22	33.06	3.55
4	88.58	0.75	58.08	2.01
5	91.15	0.74	77.55	1.04

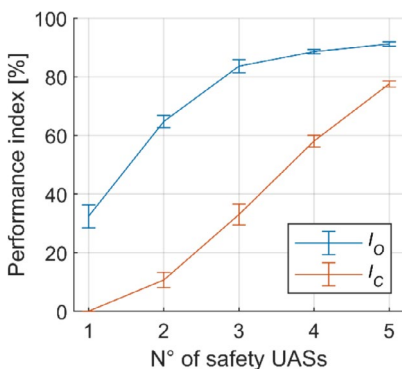


Figure 3. Graphical description of the performance indices  $I_c$  and  $I_o$  expressed in percentage as the UAS-swarm size increases.

## Discussion

The results suggest that coverage index increases as the number of safety UAS in the swarm grows, demonstrating that more safety UAS provide better coverage of the safety area around the operating UGV. However, when more than 3 safety UASs are employed, an inflection on the coverage index curve occurs, indicating that the coverage index gain decreases as the number of UAS increases. Furthermore, as more safety UAS are introduced into the swarm, the overlapping index increases, resulting in a higher redundancy.

Interestingly, the trade-off between coverage and overlap highlights an important consideration for optimizing the swarm size: while adding more UAS increases coverage, it also raises redundancy, which may lead to unnecessary resource usage. According to the results, a system made of 3 safety UAS can be considered an effective compromise of coverage and overlapping indices, since additional UAS contribute only slightly to improving the coverage index, but they increase the overlapping index (redundancy), which indicates that the added resources may not be as effective in improving the overall system efficiency.

## Conclusions

In this study, the effectiveness of deploying a UAS swarm-based surveillance system for UGV safety functionality is assessed by a simulation framework, specifically developed for a vineyard case study. The adoption of more than a single safety UAS, in swarm scheme, was envisaged and investigated to ensure a total coverage of the area, overcoming the limits due to view occlusions due to 3D crops. Results of simulations performed showed that a system made of 3 safety UASs is an effective solution, proving a coverage of more than 80% of the area around the operating UGV, with a limited unnecessary usage of resources. This study demonstrated the potential of a UAS-swarm based surveillance system for implementing an advanced UGV safety functionality in precision agriculture, with a particular focus on 3D crops.

This study represents a key tool for designing such systems, essential step toward their integration into future autonomous agricultural machinery, enabling safer autonomous precision farming practices.

## Acknowledgements

This study was carried out within the Agritech National Research Center and received funding from the European Union Next-GenerationEU (PIANO NAZIONALE DI RIPRESA E RESILIENZA (PNRR) – MISSIONE 4 COMPONENTE 2, INVESTIMENTO 1.4 – D.D. 1032 17/06/2022, CN00000022). This manuscript reflects only the authors' views and opinions, neither the European Union nor the European Commission can be considered responsible for them.

## References

- Aguzzi, G., Audrito, G., Casadei, R., Damiani, F., Torta, G., & Viroli, M. (2023). A field-based computing approach to sensing-driven clustering in robot swarms. *Swarm Intelligence*, 17, 27–62.
- Audrito, G. (2020). FCPP: an efficient and extensible Field Calculus framework. In *IEEE International Conference on Autonomic Computing and Self-Organizing Systems (ACSOS)*, pp 153–159.
- Beal, J., Pianini, D., & Viroli, M. (2015). Aggregate programming for the Internet of Things. *Computer*, 48(9), 22–30.
- Biglia, A., Grella, M., Bloise, N., Comba, L., Mozzanini, E., Sopegno, A., & Gay, P. (2022a). UAV-spray application in vineyards: Flight modes and spray system adjustment effects on canopy deposit, coverage, and off-target losses. *Science of The Total Environment*, 845, 157292.

- Biglia, A., Zaman, S., Ricauda Aimonino, D., Gay, P., & Comba, L. (2022b). 3D point cloud density-based segmentation for vine rows detection and localization. *Computers and Electronics in Agriculture*, 199, 107166.
- Cech, R., Zaller, J.G., Lyssimachou, A., Clausing, P., Hertoge, K., & Linhart, C. (2023). Pesticide drift mitigation measures appear to reduce contamination of non-agricultural areas, but hazards to humans and the environment remain. *Science of The Total Environment*, 854, 158814.
- Comba, L., Zaman, S., Biglia, A., Ricauda Aimonino, D., Dabbene, F., & Gay, P. (2020). Semantic interpretation and complexity reduction of 3D point clouds of vineyards, *Biosystems Engineering*, 197, 216–230.
- Donati, C., Mammarella, M., Comba, L., Biglia, A., Gay, P., & Dabbene, F. (2022). 3D distance filter for the autonomous navigation of UAVs in agricultural scenarios. *Remote Sensing*, 14(6), 1374.
- Mammarella, M., Comba, L., Biglia, A., Dabbene, F., & Gay, P. (2022). Cooperation of unmanned systems for agricultural applications: a case study in a vineyard. *Biosystems Engineering*, 223B, 81–102.
- Rejeb, A., Abdollahi, A., Rejeb, K., & Treiblmaier, H. (2022). Drones in agriculture: a review and bibliometric analysis. *Computers and Electronics in Agriculture*, 198, 107017.
- Semsch, E., Jakob, M., Pavlicek, D., & Pechoucek, M. (2009). Autonomous UAV surveillance in complex urban environments. In *IEEE International Joint Conference on Web Intelligence and Intelligent Agent Technology*, pp. 82–85.
- Wang, L., Lan, Y., Zhang, Y., Zhang, H., Tahir, M.N., Ou, S., Liu, X., & Chen, P. (2019). Applications and prospects of agricultural unmanned aerial vehicle obstacle avoidance in China. *Sensors*, 19(3), 642.